DALTON
FULL PAPER

Kinetic control of reactions of a sterically hindered platinum picoline anticancer complex with guanosine 5′-monophosphate and glutathione

Yu Chen, Zijian Guo, John A. Parkinson and Peter J. Sadler *

Department of Chemistry, University of Edinburgh, King's Buildings, West Mains Road, Edinburgh, UK EH9 3JJ

Received 19th August 1998, Accepted 11th September 1998

Kinetic studies (296 K, 0.1 M $NaClO_4$, pH 6–7) of reactions of the anticancer complex *cis*-[$PtCl_2(NH_3)$(2-pic)] **1** (AMD473) (2-pic = 2-picoline) with guanosine 5′-monophosphate (5′-GMP) and the tripeptide glutathione (GSH) using 2D [^1H, ^{15}N] HSQC NMR spectroscopy have been made, and compared to reactions of the isomeric complex *cis*-[$PtCl_2(NH_3)$(3-pic)] **2**. Reactions with 5′-GMP followed two pathways with either hydrolysis *trans* to NH_3 or picoline as the first step, with subsequent formation of Cl/GMP and H_2O/GMP intermediates, and *cis*-[$Pt(^{15}NH_3)$(pic)(5′-GMP-*N7*)$_2$]$^{2+}$ as the final product. Eight rate constants were determined for each starting platinum complex **1** and **2**. The rates of ligand substitution (Cl^- by H_2O and H_2O by 5′-GMP) *cis* to 2-picoline were 2–12 times slower than the same ligand substitution *cis* to 3-picoline. This was also the case for ligand substitution *trans* to 2-picoline (2–3 times slower), except that when 5′-GMP was present as the *cis* ligand (second stage of substitution) the rate of substitution was enhanced for the 2-picoline complex. Slow rotation about the Pt–N picoline bond (0.62 s^{-1}) and fast rotation about Pt-N7 GMP bonds on the NMR timescale were observed at 296 K for the bis(GMP) adduct of complex **1**, while these were both fast for the analogous adduct of complex **2**. Reactions of GSH with **1** were *ca.* 3 times slower than those with **2**, and appeared to proceed *via* aquated intermediates with initial substitution *trans* to 2-picoline for **1** and *trans* to NH_3 for **2**, but no kinetic analyses were attempted due to the complexity of the reactions. Both mono- and bis-GMP adducts were observed during competitive reactions of GSH and 5′-GMP with complex **1** (molar ratio: 2 : 2 : 1) at pH 7, 296 K. These features of the chemistry of **1** may play an important role in its altered spectrum of biological activity compared to cisplatin.

Introduction

Cisplatin, *cis*-[$PtCl_2(NH_3)_2$], is a widely used anticancer drug. Because of its serious toxic side-effects and the spontaneous development of drug resistance in tumours, there is a need for new drugs which circumvent these drawbacks. Investigations have been made of the activity of many other platinum complexes, most of which belong to the structural class *cis*-[PtX_2(ammine)$_2$] (X = anionic leaving group; ammine = ammonia, primary or secondary amine).[1] An exception is the 2-picoline (2-methylpyridine) complex *cis*-[$PtCl_2(NH_3)$(2-pic)] **1** (AMD473), which is currently in phase I clinical trials.[2,3] It possesses activity against cisplatin-resistant cell lines and against an acquired cisplatin-resistant subline of a human ovarian carcinoma xenograph both by injection and by oral administration.[2] It appears to circumvent thiol-mediated resistance mechanisms whilst still maintaining the ability to form cytotoxic lesions with DNA.[3,4] In order to gain an understanding of the chemical reactivity of this complex, we have recently investigated its crystal structure and hydrolysis behaviour in comparison with the isomeric 3-picoline complex *cis*-[$PtCl_2(NH_3)$(3-pic)] **2**.[5] The most notable feature of the structures is the orientation of the picoline ring with respect to the platinum square plane. The 2-picoline ligand is almost perpendicular (103°) such that the 2-methyl group lies directly over the square plane, while the 3-picoline ligand is tilted by 49°. This steric effect plays an important role in determining the hydrolysis rates of the Cl^- ligands. For complex **2** the rate of hydrolysis of Cl^- *trans* to NH_3 is similar to that of cisplatin ($t_{1/2}$ = 1.75 h, 310 K),[6] while for complex **1** the rate of hydrolysis for the Cl^- ligand *trans* to NH_3 (*cis* to 2-picoline) is about 5 times slower ($t_{1/2}$ = 8.7 h). The slow hydrolysis of **1** can be attributed to the axial steric hindrance provided by the 2-methyl group. Complex **1** appears to form interstrand DNA cross-links and to bind to plasma proteins much more slowly than cisplatin.[7]

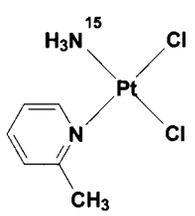

1

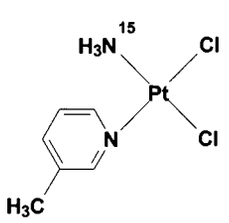

2

Besides steric effects, electronic factors may also play a role in determining the reactivity of pyridine complexes. For example the presence of planar pyridine ligands in *cis*- or *trans*-[$PtCl_2(py)_2$] complexes can reduce the rates of DNA binding compared to ammine complexes.[8] DNA platination is a key event in the mechanism of action of platinum anticancer drugs, and the major adduct formed by attack of cisplatin on DNA is the intrastrand cross-link between N7 atoms of two adjacent guanine (G) residues.[1] However, platinum can also interact with many other biomolecules, especially those containing methionine and cysteine residues. Glutathione (GSH), a cysteine-containing tripeptide (γ-L-Glu-L-Cys-Gly), is the predominant intracellular thiol with concentrations typically ranging from 0.5 to 10 mM. At physiological pH, platinum(II) complexes usually show a kinetic preference for the thiols

cysteine and glutathione over 5′-GMP, even in the presence of excess of nucleotide.[9] Reactions of thiols with platinum complexes are often considered to have a negative effect on antitumor activity and to be responsible for drug inactivation and the development of drug resistance.[10] GSH is over-expressed in cisplatin-resistant cells and Pt–GS adducts can be pumped out of cells.[11]

In this work we have investigated reactions of complex **1** and the less-hindered isomeric complex **2** with 5′-GMP and glutathione by both 1D ^{1}H and 2D [^{1}H, ^{15}N] HSQC (hetero-nuclear single quantum coherence) NMR spectroscopy, in order to investigate the influence of both steric and electronic effects on reactions of potential biological importance.

Experimental

Materials

2- and 3-Picoline and GSH were purchased from Aldrich. The sodium salt of 5′-GMP was obtained from Sigma. The complex *cis*-[$PtCl_2(^{15}NH_3)_2$] was prepared according to the reported procedure.[12] The ^{15}N labelled complexes **1** and **2** were prepared from *cis*-[$PtCl_2(^{15}NH_3)_2$] by a similar procedure to that described in the literature for natural abundance mixed-ligand ammine–amine platinum(II) complexes.[13] The diaqua complex *cis*-[$Pt(NH_3)$(2-pic)$(H_2O)_2]^{2+}$ was prepared *in situ* by addition of slightly less than 2 mol equivalents of $AgNO_3$ to an aqueous solution of complex **1** followed by removal of the AgCl precipitate.

NMR spectroscopy

The NMR spectra were recorded on a Bruker DMX500 spectrometer operating at 500.13 MHz using a TBI probehead. All data processing, including the integration routines described below, was carried out using XWIN-NMR, version 1.3 (Bruker Spectrospin Ltd.). The chemical shift references were as follows: 1,4-dioxane (internal, δ 3.767) for ^{1}H, and 1 M $^{15}NH_4Cl$ in 1.5 M HCl for ^{15}N (external). All spectra were recorded at 296 K unless otherwise stated. Typical acquisition conditions for ^{1}H spectra were: 45–60° pulses, 2.5 s relaxation delay, 64–256 transients, final digital resolution 0.2 Hz per point. The water resonance was suppressed by presaturation, or *via* the WATERGATE pulsed-field-gradient sequence.[14] The 2D [^{1}H, ^{15}N] HSQC NMR spectra (optimised for $^1J_{NH}$ = 72 Hz) were recorded by using the sequence of Stonehouse *et al.*[15] The ^{15}N spins were decoupled by irradiating with the GARP-1 decoupling sequence during acquisition. The 2D exchange experiment was performed using phase-sensitive nuclear Overhauser effect spectroscopy (NOESY) with a mixing time 1 s, at 296 K. Rates were calculated using the program D2DNMR kindly supplied by Dr K. G. Orrell.[16] Inputs for each calculation consisted of volume integrals from diagonal- and cross-peaks together with population estimates based on 1D ^{1}H NMR spectra.

All samples were in 90% H_2O–10% D_2O (0.6 ml). The reactions of complex **1** or **2** (3 mM) with 5′-GMP were conducted at a 1:2 molar ratio. Samples contained 0.1 M $NaClO_4$ to maintain a constant ionic strength. Buffer was not used in the reactions of complexes **1** and **2** with 5′-GMP in order to avoid possible interference, and the pH values were adjusted to 6.85 and 6.55 (for complexes **1** and **2**, respectively) at the beginning of the reaction. The pH value for the reaction of [$Pt(NH_3)$-(2-pic)$(H_2O)_2]^{2+}$ with 5′-GMP (1:2) was adjusted to 6.47. In the reactions of complex **1** or **2** with GSH (3 mM, 1:1 molar ratio), 100 mM phosphate buffer (pH 7) was used. Competitive reactions between 5′-GMP and GSH with complexes **1** or **2** (2 mM) were carried out at 2:2:1 molar ratios, with 100 mM phosphate buffer present to maintain neutral pH. After mixing, argon was bubbled through the solution to minimise GSH oxidation and the NMR samples were carefully sealed.

pH Measurements

These were made using a Corning 145 pH meter equipped with an Aldrich micro combination electrode calibrated with Aldrich buffer solutions of pH 4, 7 and 10. Values of pH were adjusted with 1 M $HClO_4$ or NaOH as appropriate.

Kinetic measurements

For kinetic analysis of NMR spectra, peak volumes were measured and the relative concentrations of each species were calculated at each time point. The appropriate differential equations were integrated numerically, and the rate constants were determined by a non-linear optimisation procedure using the program SCIENTIST (version 2.01, MicroMath Inc.). The errors represent one standard deviation.

Results

Labelling the ammine ligand with ^{15}N, allowed investigation of the specificity and rates of substitution of the chloride ligands in complexes **1** and **2** by 5′-GMP and GSH to be made for the first time using 2D [^{1}H, ^{15}N] NMR spectroscopy. The ^{15}N chemical shift is diagnostic of the co-ordinating atom of the ligand in the position *trans* to the ammine.[17] For an ammine ligand *trans* to an oxygen donor in a platinum(II) complex, the ^{15}N shift lies between δ −75 and −90, for an ammine *trans* to nitrogen/chloride, between δ −55 and −70, and for ammine *trans* to sulfur, between δ −40 and −50.

Reactions of complexes 1 and 2 with 5′-GMP

Both 1D ^{1}H and 2D [^{1}H, ^{15}N] HSQC NMR spectroscopy were used to monitor the reactions between complex **1** or **2** (3 mM) and 5′-GMP in a 1:2 molar ratio at 296 K and pH 6.85 or 6.55, respectively. The 2D [^{1}H, ^{15}N] HSQC NMR spectra recorded 40 h after mixing for complex **1** and 20 h for complex **2** are shown in Fig. 1A and 1B, respectively. For the 3-picoline complex **2**, the peak assignable to **2** at δ 4.26/−62.68 (peak **2a**) was accompanied by two new peaks (**2b** and **2c**) with chemical shifts of δ 4.12/−79.62 and 4.33/−61.31 after 1 h. The ^{15}N shift of the former peak is typical of NH_3 *trans* to O and is consistent with assignment to [$PtCl(^{15}NH_3)$(3-pic)$(H_2O)]^+$ **2b**,[5] and the latter peak to the aqua complex **2c** with $^{15}NH_3$ *trans* to Cl, Table 1 (for the structures of complexes, see Scheme 1). The intensity of the cross-peak from the monoaqua complex **2b**, in which the H_2O is *trans* to NH_3, is much stronger than that of complex **2c** with H_2O *trans* to 3-picoline. After 2 h, two other new peaks (**2d** and **2e**) appeared at δ 4.27/−64.21 and 4.53/−60.81, which are both in the region of $^{15}NH_3$ *trans* to N or Cl. By comparing the intensities of these two peaks with those for the two monoaqua species (**2b**, **2c**), the stronger cross-peak **2d** can be assigned to [$PtCl(^{15}NH_3)$(3-pic)(5′-GMP-*N7*)]$^+$ (GMP *trans* to NH_3), and cross-peak **2e** to [$PtCl(^{15}NH_3)$-(3-pic)(5′-GMP-*N7*)]$^+$ (GMP *trans* to 3-picoline). These two peaks reached a maximum intensity after 5 to 6 h and then gradually decreased in intensity. Cross-peaks **2f** at δ 4.44/−60.93 (NH_3 *trans* to N) and **2g** at δ 4.47/−75.92 (NH_3 *trans* to O) differ greatly in intensity, comparable to the difference observed for cross-peaks **2d** and **2e** (Fig. 1B). Therefore, cross-peak **2f** is assignable to [$Pt(^{15}NH_3)$(3-pic)(5′-GMP-*N7*)$(H_2O)]^{2+}$ (GMP *trans* to NH_3) and cross-peak **2g** to [$Pt(^{15}NH_3)$(3-pic)-(5′-GMP-*N7*)$(H_2O)]^{2+}$ (GMP *trans* to 3-picoline). Cross-peak **2h** at δ 4.63/−62.60, which was observable from soon after the beginning of the reaction, increased in intensity with time, and became the major cross-peak after 24 h. This is assignable to the final bis 5′-GMP product *cis*-[$Pt(^{15}NH_3)$(3-pic)(5′-GMP-*N7*)$_2]^{2+}$ **2h**. An unassigned cross-peak **2i** at δ 4.33/−59.55 appeared after 8 h of reaction, but accounted for only a very small amount of the total Pt–NH_3 species present (<4%), and

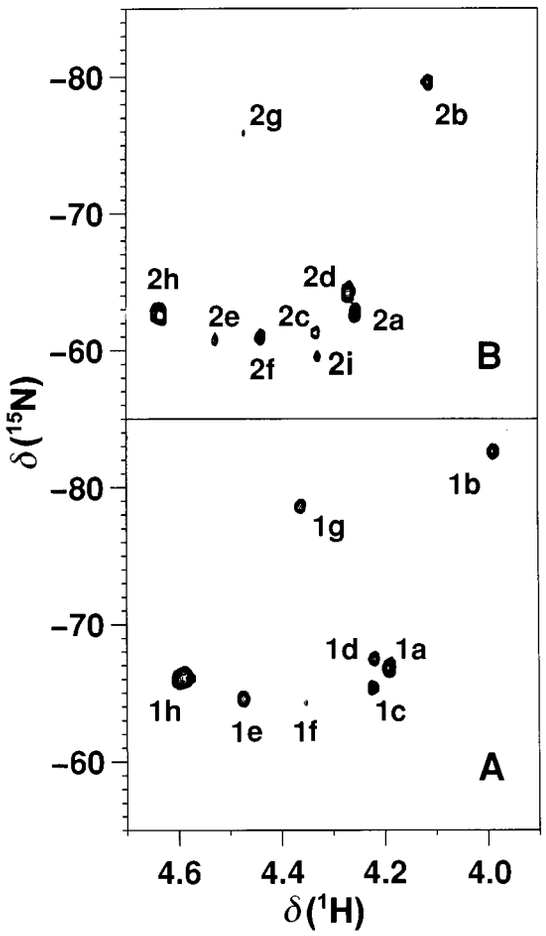

Fig. 1 The 2D [^{1}H, ^{15}N] HSQC NMR spectra from reactions of 2 mol equivalents of 5′-GMP (0.1 M $NaClO_4$, 296 K) with (A) ($^{15}NH_3$)-**1**, pH 6.85, after 40 h and (B) ($^{15}NH_3$)-**2** pH 6.55, after 20 h. Peak assignments are given in Table 1.

Table 1 Proton and ^{15}N NMR Pt–NH_3 chemical shifts at 296 K for *cis*-[Pt($^{15}NH_3$)(2-pic)]$^{2+}$ and *cis*-[Pt($^{15}NH_3$)(3-pic)]$^{2+}$ complexes

Compound	Peak *	δ(^{1}H)	δ(^{15}N) ($^{15}NH_3$ *trans* to)
[$PtCl_2$($^{15}NH_3$)(2-pic)]	**1a**	4.19	−66.75 (Cl)
[PtCl($^{15}NH_3$)(2-pic)(H_2O)]$^+$	**1b**	3.99	−82.61 (O)
[PtCl($^{15}NH_3$)(2-pic)(H_2O)]$^+$	**1c**	4.23	−65.34 (Cl)
[PtCl($^{15}NH_3$)(2-pic)(5′-GMP-*N7*)]$^+$	**1d**	4.22	−67.43 (N)
[PtCl($^{15}NH_3$)(2-pic)(5′-GMP-*N7*)]$^+$	**1e**	4.47	−64.51 (Cl)
[Pt($^{15}NH_3$)(2-pic)(5′-GMP-*N7*)(H_2O)]$^{2+}$	**1f**	4.35	−64.18 (N)
[Pt($^{15}NH_3$)(2-pic)(5′-GMP-*N7*)(H_2O)]$^{2+}$	**1g**	4.36	−78.60 (O)
[Pt($^{15}NH_3$)(2-pic)(5′-GMP-*N7*)$_2$]$^{2+}$	**1h**	4.59	−65.87 (N)
		4.58	−66.15 (N)
[$PtCl_2$($^{15}NH_3$)(3-pic)]	**2a**	4.26	−62.68 (Cl)
[PtCl($^{15}NH_3$)(3-pic)(H_2O)]$^+$	**2b**	4.12	−79.62 (O)
[PtCl($^{15}NH_3$)(3-pic)(H_2O)]$^+$	**2c**	4.33	−61.31 (Cl)
[PtCl($^{15}NH_3$)(3-pic)(5′-GMP-*N7*)]$^+$	**2d**	4.27	−64.21 (N)
[PtCl($^{15}NH_3$)(3-pic)(5′-GMP-*N7*)]$^+$	**2e**	4.53	−60.81 (Cl)
[Pt($^{15}NH_3$)(3-pic)(5′-GMP-*N7*)(H_2O)]$^{2+}$	**2f**	4.44	−60.93 (N)
[Pt($^{15}NH_3$)(3-pic)(5′-GMP-*N7*)(H_2O)]$^{2+}$	**2g**	4.47	−75.92 (O)
[Pt($^{15}NH_3$)(3-pic)(5′-GMP-*N7*)$_2$]$^{2+}$	**2h**	4.63	−62.60 (N)
Unassigned	**2i**	4.33	−59.55 (N)

* See Fig. 1.

disappeared after 1 week. The assignments and chemical shifts of all peaks are listed in Table 1. The reaction pathway is summarised in Scheme 1.

The reaction of the 2-picoline complex **1** with 5′-GMP was much slower in comparison with complex **2**. Only peaks for

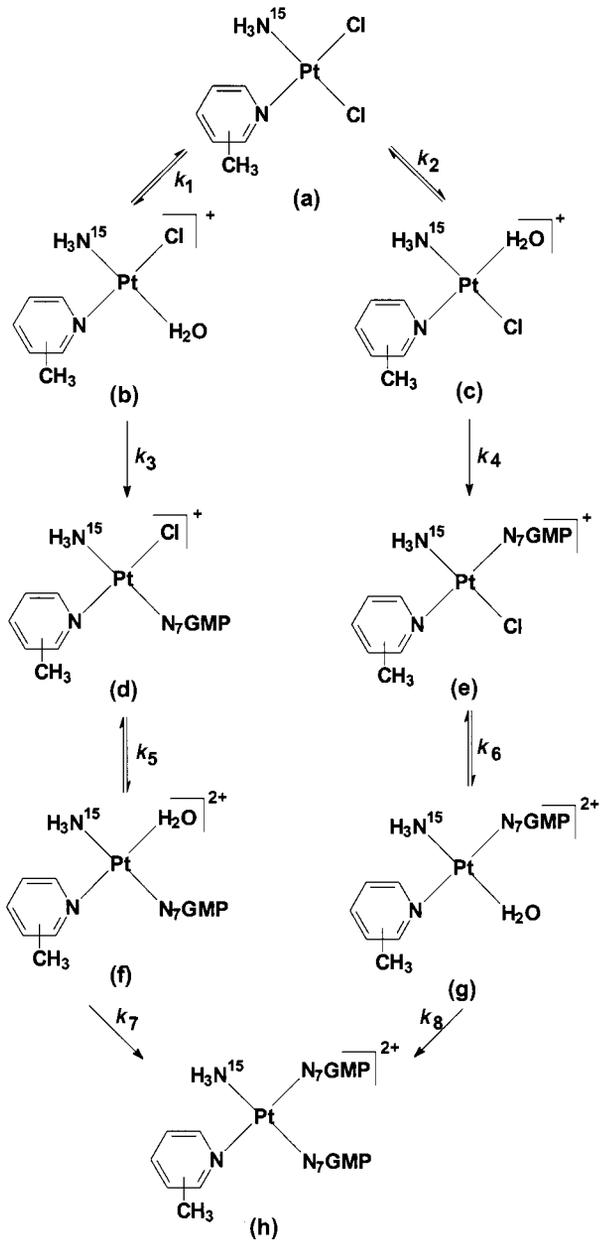

Scheme 1

complex **1** (peak **1a**) (δ 4.19/−66.75) and two monoaqua hydrolysis adducts (peaks **1b** and **1c**) with similar intensity (δ 3.99/−82.61, 4.23/−65.34, respectively) were observed after 2 h at 296 K. The chemical shift distribution of the cross-peaks for the 2-picoline complexes in Fig. 1A is very similar to that for the 3-picoline complexes in Fig. 1B, except that all the ^{15}N chemical shifts of the signals in Fig. 1B are shifted to low frequency by *ca.* 3 ppm. However, the relative intensities of the cross-peaks for the intermediates in the reaction of complex **1** with 5′-GMP are different from those for complex **2**. Cross-peaks **1e** at δ 4.47/−64.51 and **1g** at δ 4.36/−78.60 are stronger than the peaks **1d** at δ 4.22/−67.43 and **1f** at δ 4.35/−64.18, respectively, whereas, for complex **2**, cross-peaks **2d** and **2f** are much stronger than **2e** and **2g**. The two cross-peaks **1b** and **1c** for the monoaqua adducts of complex **1** had similar intensities during the reaction. The final bis(GMP) adduct is formed much more slowly for complex **1** compared to complex **2**. The broad cross-peak (**1h**) for the bis(GMP) adduct of complex **1** appeared to be composed of two overlapping cross-peaks at δ 4.59/−65.96 and 4.58/−66.15. The peak intensity *versus* time profiles (Fig. 2) allowed similar assignments to be made for the cross-peaks obtained from reactions between complexes **1**

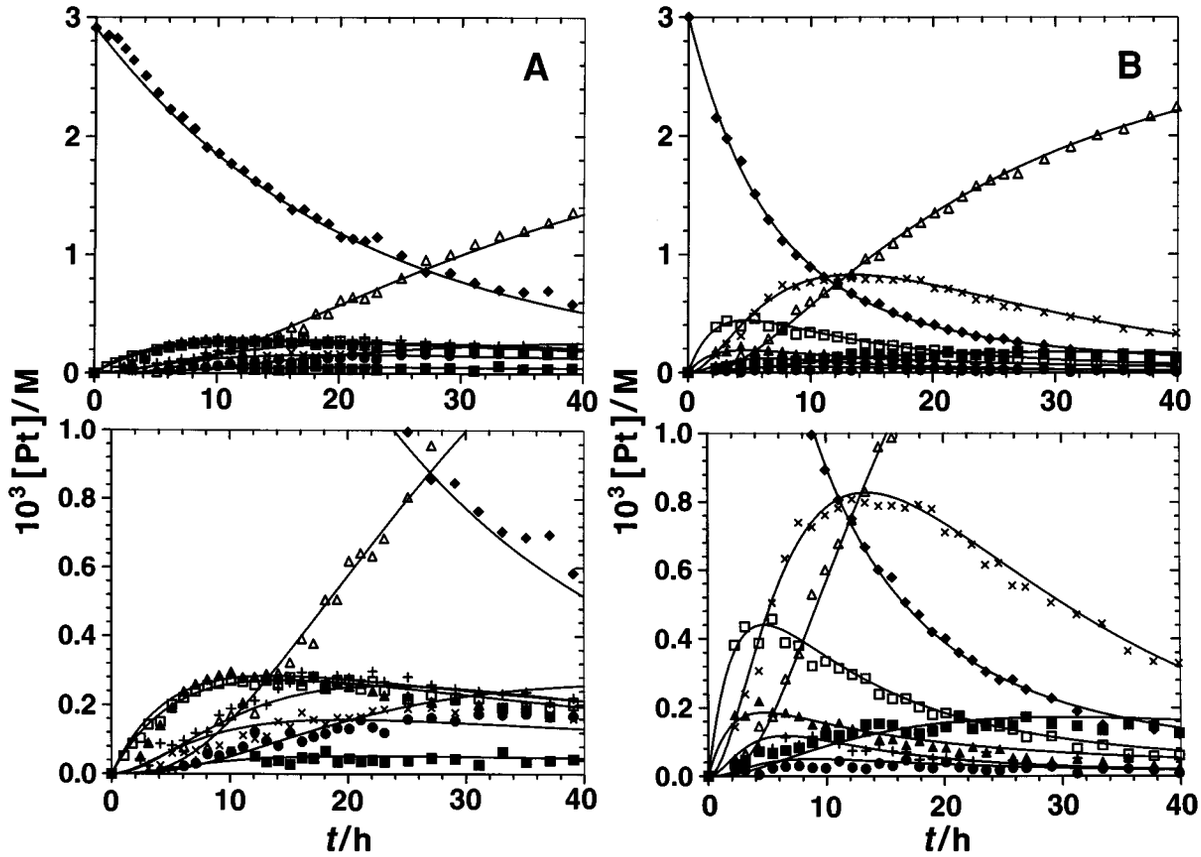

Fig. 2 Plots of the relative concentrations of species **a** to **h** (based on Pt–NH_3 peak integrals) *versus* time for the reactions shown in Fig. 1. (A) 2-Picoline complex **1**, (B) 3-picoline complex **2**. Peak labels: (**a**) ◆, (**b**) □, (**c**) ▲, (**d**) ×, (**e**) +, (**f**) ■, (**g**) ●, (**h**) △. The curves are the computer best fits for the rate constants given in Table 2.

Table 2 Rate constants for reactions of *cis*-[PtCl(NH_3)(pic)] with 5′-GMP at 296 K (0.1 M $NaClO_4$). The errors represent one standard deviation

Rate constants	Complex		Ratio $k_{3\text{-pico}}/k_{2\text{-pico}}$
	2-Picoline	3-Picoline	
k_1/s^{-1}	$6.87 (\pm 0.18) \times 10^{-6}$	$2.60 (\pm 0.03) \times 10^{-5}$	4
k_2/s^{-1}	$5.87 (\pm 0.18) \times 10^{-6}$	$1.17 (\pm 0.03) \times 10^{-5}$	2
$k_3/M^{-1}\ s^{-1}$	$7.97 (\pm 0.33) \times 10^{-3}$	$1.60 (\pm 0.03) \times 10^{-2}$	2
$k_4/M^{-1}\ s^{-1}$	$6.67 (\pm 0.37) \times 10^{-3}$	$1.87 (\pm 0.08) \times 10^{-2}$	3
k_5/s^{-1}	$8.53 (\pm 1.11) \times 10^{-5}$	$1.78 (\pm 0.04) \times 10^{-5}$	0.2
k_6/s^{-1}	$2.77 (\pm 0.31) \times 10^{-5}$	$1.48 (\pm 0.14) \times 10^{-4}$	5
$k_7/M^{-1}\ s^{-1}$	$4.2 (\pm 0.6) \times 10^{-2}$	$3.2 (\pm 0.1) \times 10^{-2}$	0.8
$k_8/M^{-1}\ s^{-1}$	$5.92 (\pm 0.74) \times 10^{-3}$	$6.85 (\pm 0.75) \times 10^{-2}$	12

and **2** with 5′-GMP (Table 1). Cross-peaks **1g**, **1f** and **1h** were also observed during reaction of the diaqua complex *cis*-[Pt($^{15}NH_3$)(2-pic)(H_2O)$_2$]$^{2+}$ (3 mM) with 5′-GMP (1 : 2) at 296 K and pH 6.47.

Kinetic fits to the reaction profile in Scheme 1 for complexes **1** and **2** are shown in Fig. 2A and 2B, and the rate constants for each step are listed in Table 2. Most of the rate constants for the reaction steps of complex **2** with 5′-GMP are more than twice as large as those for complex **1**, except k_5 and k_7. The largest differences are for k_6 and k_8 (substitution of Cl^- *cis* to picoline by H_2O, and then by 5′-GMP in the second stage), which are five and twelve times larger for complex **2**.

Rotation of 5′-GMP and 2-picoline in *cis*-[Pt(NH_3)(2-pic)-(5′-GMP)$_2$]$^{2+}$

The ^1H NMR spectra for the reactions between complex **1** or **2** and 5′-GMP (1 : 2 reaction ratio) at 296 K recorded after 2 h and 1 week are shown in Fig. 3. For complex **1**, after 1 week of reaction, the H8 resonance of free 5′-GMP at δ 8.19 and the methyl signal of complex **1** at δ 3.15 have completely disappeared (Fig. 3A). Four major H8 signals were observed in two sets of two singlets between δ 8.7 and 8.3, and two methyl signals appeared at δ 3.30 and 3.27. The H1′ signals of bound 5′-GMP were also observed in two sets of two doublets, with vicinal coupling constants ^3J(H1′–H2′) = 4.8, 4.4 and 5.1, 4.9 ± 0.1 Hz. However, for complex **2** after 1 week of reaction, only two H8 signals at δ 8.66 and 8.52 were observed together with one methyl signal at δ 2.36 and two H1′ doublets [^3J(H1′–H2′) = 4.6 and 4.9 ± 0.1 Hz] for bound 5′-GMP (Fig. 3B). The ^1H NMR data for *cis*-[Pt(NH_3)(2-pic)(5′-GMP)$_2$]$^{2+}$ **1h** and *cis*-[Pt(NH_3)(3-pic)(5′-GMP)$_2$]$^{2+}$ **2h** are listed in Table 3. The temperature dependence of the H8 signals of [Pt(NH_3)-(2-pic)(5′-GMP)$_2$]$^{2+}$ is shown in Fig. 4. The four H8 singlets coalesced into two singlets when the temperature was raised to 338 K. Based on the coalescence temperature (T_c) and the chemical shift differences ($\Delta\nu$ in Hz) between the two signals in the slow exchange limit, a rate constant k_c of 25.5 s^{-1} ($k_c = 2.22\ \Delta\nu$) and activation free energy $\Delta G^{\ddagger}$ of 73.2 kJ mol^{-1} for the exchange process at 338 K were calculated.[18] At 338 K, the two ^1H, ^{15}N cross-peaks which constituted peak **1h** (Fig. 1A) for bis(GMP) adducts of complex **1** merged into one cross-peak. The two methyl signals at δ 3.30 and 3.27 also became closer when the temperature was raised to over 333 K. Because of the temperature limitation of the NMR probe, the spectrum was recorded at a maximum temperature of 348 K, where no coalescence of the two methyl signals was observed. When the spectra were recorded at 250 MHz the two methyl signals were observed to coalescence at 343 K, from which similar k_c (25.6 s^{-1}) and $\Delta G^{\ddagger}$ (75.15 kJ mol^{-1}) values were obtained. A 2D EXSY (exchange spectroscopy) experiment with a mixing time of 1 s (Fig. 5) showed clear exchange cross-peaks between the

Table 3 ^{1}H Chemical shifts and coupling constants (Hz) for bis(5′-GMP) adducts of complexes **1** (pH 6.85) and **2** (pH 6.55) at 296 K

Complex	δ H8	δ CH_3	δ H1′	^3J(H1′–H2′)/Hz
1 *cis*-$[PtCl_2(NH_3)(2\text{-pic})]$		3.15		
$[Pt(NH_3)(2\text{-pic})(5'\text{-GMP})_2]^{2+}$	8.66, 8.63	3.30, 3.27	5.93, 5.92	4.8, 4.4
	8.42, 8.40		5.80, 5.78	5.1, 4.9
2 *cis*-$[PtCl_2(NH_3)(3\text{-pic})]$		2.37		
$[Pt(NH_3)(3\text{-pic})(5'\text{-GMP})_2]^{2+}$	8.66, 8.52	2.36	5.93, 5.82	4.6, 4.9

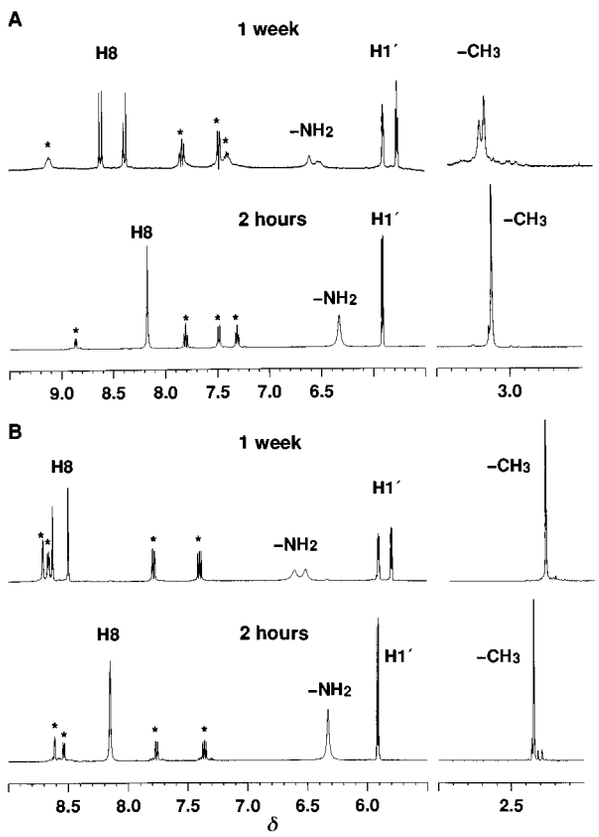

Fig. 3 The ^{1}H NMR spectra recorded after 2 h and 1 week of reactions at 296 K of 5′-GMP (2 mol equivalents) with (A) complex **1** and (B) complex **2**. The peaks labelled * are from the aromatic protons of picoline ligands.

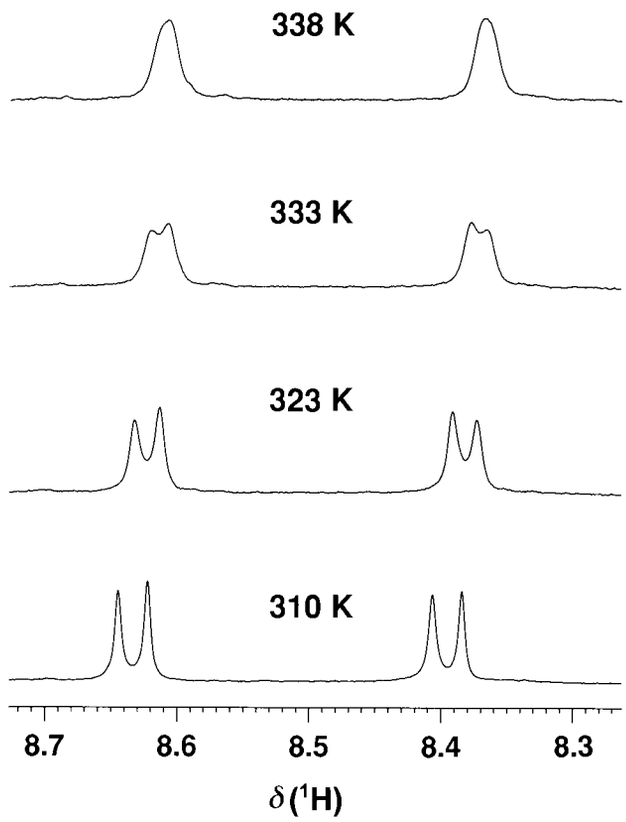

Fig. 4 The temperature dependence of the H8 ^{1}H NMR signals of *cis*-$[Pt(NH_3)(2\text{-pic})(5'\text{-GMP})_2]^{2+}$.

two methyl signals at 296 K. An average rate constant for the exchange process of 0.62 s^{-1} at this temperature was determined. Interestingly, one of the four H8 signals at δ 8.42 (Fig. 3A) for the bis(GMP) adduct of complex **1** became broader when the temperature was below 296 K, as did one of the CH_3 signals at δ 3.30.

Reactions of complexes 1 and 2 with glutathione (1 : 1, pH 7)

Reactions of complexes **1** and **2** with GSH were followed by 2D [^{1}H, ^{15}N] HSQC NMR spectroscopy. Spectra recorded after 3.5 h are shown in Fig. 6. In both cases, peaks assignable to hydrolysis products (**1b**, **1c** and **2b**, **2c**) were observed before the appearance of peaks for GSH adducts. For complex **2**, cross-peaks from GSH adducts began to appear after 45 min in the δ(^{15}N) region of −35 to −40 which corresponds to NH_3 *trans* to S, while for complex **1** new peaks were observed only after 2 h and in the δ(^{15}N) region of −62 to −67 which corresponds to NH_3 *trans* to N or Cl. Therefore, the first binding site for GS^- is *trans* to 2-picoline for complex **1**, but *cis* to 3-picoline for complex **2**. Due to the complicated nature of the reactions (Table 4), no specific assignments for the products of the reactions between complex **1** and **2** and GSH have been made. Time

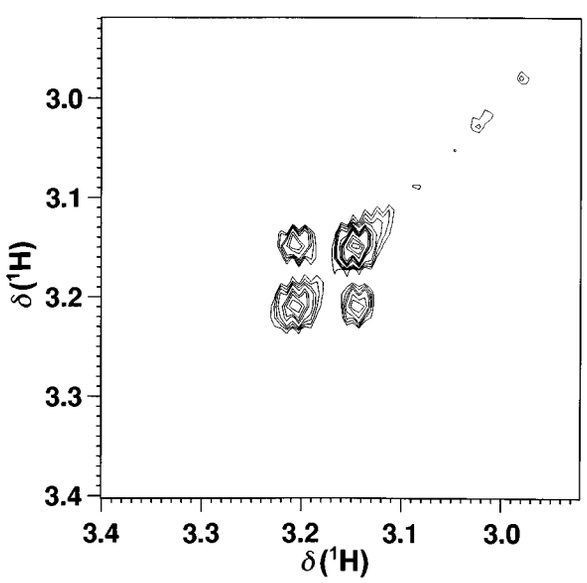

Fig. 5 The 2D EXSY spectrum (mixing time = 1 s) for *cis*-$[Pt(NH_3)(2\text{-pic})(5'\text{-GMP})_2]^{2+}$ showing exchange cross-peaks between the two methyl signals, indicative of the slow rotation of co-ordinated 2-picoline.

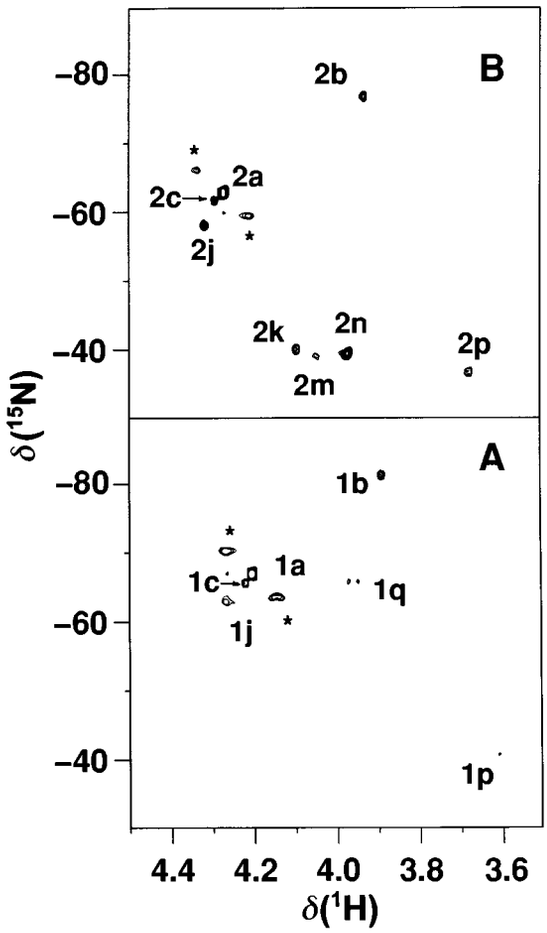

Fig. 6 Two-dimensional [^{1}H, ^{15}N] HSQC NMR spectra for reactions of GSH (1 mol equivalent) with (A) complex **1** and (B) complex **2**, recorded at 296 K, pH 7 (100 mM phosphate buffer) after 3.5 h. Peaks (**1a** to **1c**, and **2a** to **2c**) are assigned according to Table 1; the others are unassigned. Satellites (^{195}Pt) of peaks **1a** and **2a** are labelled with *. Peaks with ^{15}N chemical shifts near δ −40 are characteristic of NH_3–Pt *trans* to sulfur.

Table 4 Proton and ^{15}N NMR Pt–NH_3 chemical shifts at 296 K for the major peaks observed during the reactions of complexes **1** and **2** with GSH (1 : 1 molar ratio, pH 7)

Peak[a]	δ(^{1}H)	δ(^{15}N) ($^{15}NH_3$ *trans* to)
1a	4.21	−66.84 (Cl)
1b	3.89	−81.27 (O)
1c	4.23	−65.49 (Cl)
1j	4.27	−62.64 (N or Cl)
1p	3.60	−40.85 (S)
1q	3.97, 3.95	−65.84, −65.95 (N or Cl)
*	4.29	−62.52 (N or Cl)
*	4.25	−62.89 (N or Cl)
*	3.96	−43.24 (S)
*	4.05	−42.76 (S)
*	3.69	−42.12 (S)
2a	4.27	−62.82 (Cl)
2b	3.93	−76.77 (O)
2c	4.30	−61.74 (Cl)
2j	4.32	−58.14 (N or Cl)
2k	4.10	−40.09 (S)
2m	4.05	−39.01 (S)
2n	3.97	−39.37 (S)
2p	3.68	−36.70 (S)

[a] For peak labels, see Fig. 6. Peaks labelled * were not observed in the same spectrum as the other peaks but appeared at later times.

dependences of the concentrations of complexes **1** and **2** and their monoaquachloro adducts during the reactions with GSH

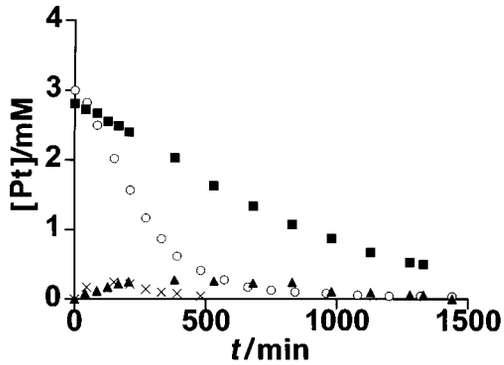

Fig. 7 Time dependence of the concentrations of the starting complex **1** (■), its monoaquachloro adducts (**1b** + **1c**) (▲), and complex **2** (○), its monoaquachloro adducts (**2b** + **2c**) (×), during reactions with GSH (1 : 1 molar ratio, pH 7, 296 K).

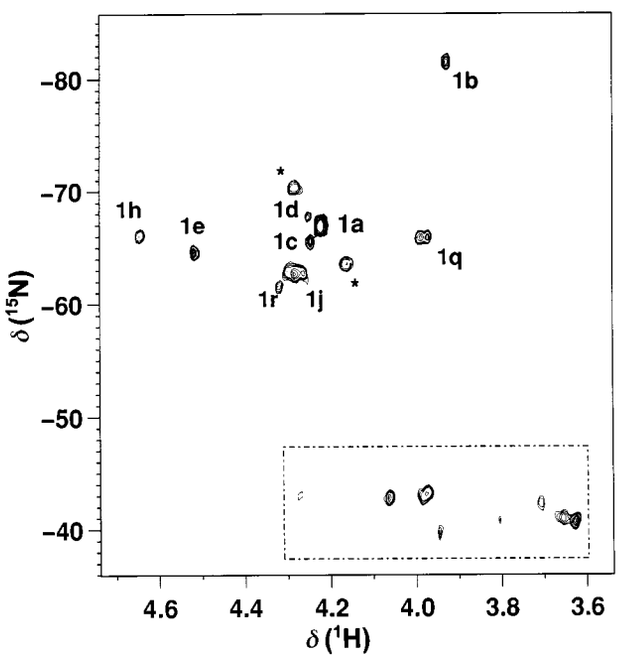

Fig. 8 The 2D [^{1}H, ^{15}N] HSQC NMR spectra for the competitive reaction of GSH and 5′-GMP with complex **1** (molar ratio: 2 : 2 : 1) at 296 K, pH 7.0 (100 mM phosphate buffer) recorded after 14.5 h. Peaks of 5′-GMP adducts (**1d**, **1e**, **1h**) and GSH adducts (**1j**, **1q**) are labelled according to those in Tables 1 and 4. Satellites of peak **1a** are labelled with *. The peaks in the dashed box are due to the formation of GSH adducts (^{15}N chemical shifts near δ −40 are characteristic of NH_3–Pt *trans* to sulfur), but no specific assignments were made. Peak **1r** is tentatively assigned to an adduct with one GMP and one GSH ligand in the *cis* position (NH_3–Pt *trans* to N7).

are shown in Fig. 7. The rate of reaction of complex **2** is about 3 times as fast as that of complex **1**. After 2 weeks' standing at ambient temperature, yellow precipitates formed in both reactions, and all the signals had disappeared from the 2D [^{1}H, ^{15}N] HSQC NMR spectra.

Competitive reactions of 1 or 2 with GSH and 5′-GMP

The reaction of complex **1** with GSH in the presence of 5′-GMP (1 : 2 : 2) was followed by 2D [^{1}H, ^{15}N] NMR spectroscopy at 296 K, pH 7 (100 mM phosphate buffer). A spectrum recorded after 14.5 h of reaction is shown in Fig. 8. Only the peaks for the starting complex **1** (peak **1a**) and hydrolysis products (peaks **1b**, **1c**) were present after 0.5 h. Peak **1q**, which was also observed during the reaction with GSH (Fig. 6A), began to appear after 1 h of reaction. The mono(GMP) adduct (peak **1e**) began to form after 2.5 h, and the bis(GMP) adduct (peak **1h**) was present after 8 h of reaction. Peaks due to both 5′-GMP adducts (**1d**, **1e**, **1f** and **1h**) and GSH adducts (peaks

1q, **1j, 1r** and those in dashed box) are present in Fig. 8. Due to the complicated nature of GSH reactions, no attempt was made to assign the peaks **1q**, **1j** or those in the region for NH_3–Pt *trans* to S (dashed box, Fig. 8). Most of these peaks for GSH adducts were also observed in the reaction of complex **1** with GSH in the absence of 5′-GMP. Peak **1r** has a ^{15}N chemical shift in the region of NH_3–Pt *trans* to N or Cl, and was not observed in the reactions of **1** with 5′-GMP or with GSH. It can be tentatively assigned to a mixed-ligand adduct containing GMP *trans* to NH_3 and a GS^- ligand. Spectra recorded after 3 d of reaction at 296 K showed that only one major peak (**1h**) in the region of NH_3–Pt *trans* to N or Cl [$\delta(^{15}N)$ −60 to −70] together with some other peaks [$\delta(^{15}N)$ −40 to −45] in the region of NH_3–Pt *trans* to S. The presence of a strong H8 signal at δ 8.13 due to free 5′-GMP in 1D spectra recorded after 3 d showed that most of the 5′-GMP was still unreacted at this stage, while signals for free GSH had nearly disappeared. The 2-methyl signal at δ 3.15 from co-ordinated 2-picoline had shifted to δ 2.57, which implied that the 2-picoline ligand had been mostly displaced. Signals for the bis(GMP) adduct were only just visible in 1D spectra because of their low intensity and overlap with broad signals. Compared with **1**, the competitive reaction of **2** with GSH and 5′-GMP (1:2:2) was much faster and peaks assignable to GSH adducts were detectable after 0.5 h. Mono- and bis-GMP products started to appear after 1.5 and 5 h of reaction, respectively. Much less of the bis(GMP) adduct of complex **2** was formed in the competitive reaction with GSH compared to complex **1**.

Discussion

The complex *cis*-$[PtCl_2(NH_3)(2\text{-pic})]$ **1** is a new anticancer drug which has a different spectrum of biological activity compared to cisplatin. In particular it is active against cisplatin-resistant cell lines and xenographs.[2–4] In order to shed light on the chemical reactivity of **1**, and to elucidate the potential role of steric hindrance,[5] we have made kinetic studies of reactions of complex **1** with 5′-GMP and GSH in comparison to the isomeric 3-picoline complex **2**. By labelling complexes with $^{15}NH_3$, it was possible to determine for the first time the specificity of substitution of the chloride ligands by 5′-GMP and GSH using 2D [^1H, ^{15}N] HSQC NMR spectroscopy. Because of the sensitivity of the ^{15}N chemical shifts to the ligand *trans* to H_3N–Pt, and of ^1H NH_3 shifts to *cis* effects, it has been possible to resolve peaks for a variety of intermediates in the reactions, detect them at micromolar concentrations, and make reasonable assignments.

Reactions with 5′-GMP

Concentration *versus* time profiles for reactions of complexes **1** and **2** with 5′-GMP were fitted well by the kinetic scheme shown in Scheme 1, showing that they are two-step and two stage: initial hydrolysis followed by 5′-GMP substitution to give the 1:1 Pt–5′GMP adduct, and then further hydrolysis and 5′-GMP substitution to give the final product, the bis-(5′-GMP) complex. For each complex there are two routes to the final product, depending on whether initial substitution is *trans* to picoline or *trans* to NH_3. From the rate constants listed in Table 2, the following conclusions can be drawn.

(i) The rates of ligand substitution (Cl^- by H_2O, or H_2O by 5′-GMP) *cis* to picoline (k_1, k_3, k_6, k_8) are 2–12 times slower for the 2-picoline complexes compared to 3-picoline.

(ii) The rates of substitution *trans* to picoline are also slower for the 2-picoline complex (2–3 times slower) except when 5′-GMP is present as the *cis* ligand (compare k_5 and k_7 values for complexes **1** and **2**, Table 2). However, it should be noted that the errors for some of the rate constants determined for the second stage of the reaction are rather large on account of the low concentrations of the intermediates.

The relative rates of the first step of the GMP reactions are similar to those we determined previously for hydrolysis of the complexes, and for complex **2** these follow the order expected from the higher *trans* influence of NH_3 (pK_a 9.29) compared to 3-picoline (pK_a 6.0),[19] which is the weaker σ donor. Since 2-picoline has a similar pK_a value (6.1) to that of 3-picoline, the similarity in the hydrolysis rates for Cl^- *trans* to NH_3 and *trans* to 2-picoline in complex **1** can be attributed to steric hindrance provided by the 2-methyl group. In the crystal structure of complex **1**, the 2-picoline ligand is almost perpendicular to the platinum square plane (102.7°) and the methyl group is close to Pt ($H_3C \cdots Pt$ 3.224 Å).[5]

Such steric hindrance is well known to slow down the rates of ligand substitution reactions in square-planar metal complexes.[20] For example, the rate constants (s^{-1}) for the hydrolysis of *cis*-$[PtCl(L)(PEt_3)_2]$ complexes (the replacement of Cl^- by H_2O) decrease in the order of (L): pyridine (800×10^{-4}) > 2-methylpyridine (2.0×10^{-4}) > 2,6-dimethylpyridine (0.01×10^{-4}).[21] In the latter case the methyl groups block entry of incoming nucleophiles both above and below the square plane. The steric effect is more prominent in the position *cis* to 2-picoline which is consistent with the CH_3 group being further from the entering and leaving groups in the trigonal bipyramidal transition state if the pyridyl ligand is in the trigonal plane.[21,22] The plane of the 3-picoline ring in complex **2** is tilted by 48.9° with respect to the platinum square plane, and the rates of substitution for **2** are determined mainly by the *trans* effect.

The rate of binding of the second 5′-GMP ligand in the position *cis* to picoline is much slower for complex **1** compared with **2**, which gives rise to a long-lived monofunctional adduct for the 2-picoline complex. This may explain the brief report that complex **1** forms DNA cross-links extremely slowly.[7] There appear to be no comparable kinetic data available in the literature for reactions of 5′-GMP with cisplatin. Compared to the rate constants for the second stage of binding of 5′-GMP to $[Pt(NH_3)_2(5'\text{-GMP})(H_2O)]^{2+}$ (298 K, 0.24 M^{-1} s^{-1}),[23] those for complexes **1** and **2** are an order of magnitude smaller. The rates of reactions of aquachloro cisplatin with DNA oligonucleotides[24,25] are about two orders of magnitude faster in comparison to those for reaction of the chloroaqua species of the picoline complexes **1** and **2** with 5′-GMP.

Rotation of ligands in bis(5′-GMP) adducts

Restricted rotation about the Pt–N7 bonds can potentially lead to three different bis(GMP) stereoisomers for square-planar complexes having two *cis* ligands with C_2 local symmetry: two head-to-tail (HT) and one head-to-head (HH) species, with the H8s of 5′-GMP on the opposite side or on the same side of the platinum co-ordination plane, respectively. Because of the chiral ribose of 5′-GMP, the H/T enantiomers become diastereomers and should be distinguishable by NMR. If the *cis*-PtA_2 moiety lacks local C_2 symmetry [*e.g.* two different A (A, A′) or an unsymmetrical chelate], four different stereoisomers (two HT and two HH) are possible when there is restricted rotation about the Pt–N7 bonds in bis(GMP) complexes.[26] Normally only HT conformations are expected to be thermodynamically favoured and detectable in solution, as is found in most solid-state crystallographic studies.[27–29] Each H8 is non-equivalent for both HT stereoisomers,[28,30,31] giving a total of four H8 signals for the HT stereoisomers.[32] For the 2-picoline complex **1**, the 2-methyl group can be on the upper side or the lower side of the platinum plane for each HT stereoisomer, so theoretically eight H8 signals should be observed for the two HT isomers together with four methyl signals (Scheme 2) when there is slow rotation (on the NMR timescale) about both the Pt–N7 (GMP) and Pt–N (picoline) bonds. Usually fast rotation of bound GMP about the Pt–N7 bond in *cis*-$[PtA_2(GMP)_2]$ (where A_2 are two unidentate or

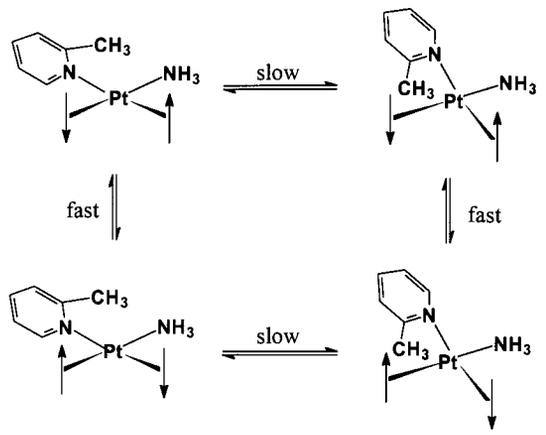

Scheme 2 Diastereomers of *cis*-[Pt($^{15}NH_3$)(2-pic)(5′-GMP-*N7*)$_2$]$^{2+}$. The arrows (⟶) represent 5′-GMP molecules, with the head of the arrow denoting H8.

one bidentate amine ligand) is expected if the substituents on the two *cis* amine ligands are not very bulky.[30,32] In our NMR experiments only four H8 signals in two sets of two singlets were observed for complex **1**, together with two methyl signals. This suggests that rotation of 5′-GMP about the Pt–N7 bond is fast on the NMR timescale but slow about the Pt–N bond for 2-picoline. This slowness of the rotation was evident from the exchange rate (0.62 s^{-1}, 296 K) determined from the 2D EXSY spectrum. The activation free energy ($\Delta G^{\ddagger}$) measured from the coalescence temperature of the H8 signals represents the barrier for rotation about the Pt–N (2-picoline) bond. The coalescence of the two close cross-peaks comprising peak **1h** in the 2D [^{1}H, ^{15}N] HSQC NMR spectrum of the bis(GMP) adduct of complex **1** at 65 °C can also be attributed to faster rotation about the Pt–N (2-picoline) bond at higher temperature. The broadening of one H8 signal and one CH_3 signal at low temperature (<296 K) suggests that one of the bound GMP ligands (probably that *cis* to 2-picoline) in a HT stereoisomer is more affected by the rotation of Pt–N (2-picoline) than the other. Compared with complex **1**, the rotation of 3-picoline in complex **2** is facile, there being little steric hindrance from the methyl group in this case. Slow rotation about Pt–N (2-picoline) bonds has been reported previously for *cis*-[Pt(2-pic)$_2$(Guo)$_2$]$^{2+}$ at room temperature, whilst the rotation about Pt–N7 (Guo) was still fast on the NMR timescale.[33]

Hydrogen-bond interactions between ammine hydrogens and O(6) or the 5′-phosphate of GMP can give rise to high-frequency ^{1}H chemical shifts of Pt–NH_3 groups in bis(GMP) adducts (**1h** and **2h**). Platinum co-ordination to nucleotides is known to induce a change in the sugar-ring conformation from S-type (C2′-*endo*) to N-type (C3′-*endo*), which changes the H1′–H2′ coupling constant,[34] consistent with the small decrease observed in the present work.

The facile rotation of guanine about the Pt–N7 bond is thought to be important in the binding of cisplatin to DNA. From the results obtained here, several isomers would be expected when complex **1** reacts with G bases of DNA because of the steric effect of 2-picoline and the non-C_2-symmetrical structure, which is similar to *cis*-[$PtCl_2(NH_3)(C_6H_{11}NH_2)$].[35] These isomers may be stabilised by different hydrogen-bonding patterns and have contrasting reactivities. Such studies may allow the further development of strategies for the systematic design of platinum antitumour complexes.

Reactions with GSH

The reactions of cisplatin and related platinum complexes with S-containing nucleophiles usually occur *via* direct substitution without prior aquation,[36] as has been observed for substitution of Cl^- by methionine, GSH and metallothionein.[37–39] However, in the reactions described here, aqua adducts were the first species observed during reactions of both complexes **1** and **2** with GSH. There could be two reasons for this: (1) reactions of complexes **1** and **2** with GSH do proceed *via* hydrolysis, or (2) because of the steric effect of the picoline ligands, binding of GSH is slowed and hydrolysis is fast enough to compete with direct substitution. Unfortunately the reactions were too complicated to allow a kinetic analysis to be carried out.

The thiolate sulfur of GSH has a high *trans* effect and this can lead to labilisation and release of the ammine ligand in the *trans* position.[40] However, despite an overall loss of general signal intensity, no cross-peak for free $^{15}NH_4^+$ was observed in the 2D spectra, probably because of fast proton exchange with H_2O at pH 7. The yellow solids formed during reactions of thiols with platinum complexes are usually thought to be sulfur-bridged polymers.[39–41] From the 2D [^{1}H, ^{15}N] HSQC NMR spectrum (Fig. 6), the initial binding site for GSH on complex **1** is in the position *trans* to 2-picoline, and attributable to the steric effect in the *cis* position, which is similar to the situation for GMP binding.

No rate constants were determined for the reactions of complexes **1** and **2** with GSH due to their complicated nature, but the time-dependent plots (Fig. 7) showed that complex **1** reacted much more slowly than complex **2**. The half life ($t_{1/2}$) of complex **1** was about three times longer than that of complex **2**.

Competitive binding of GSH and 5′-GMP

At neutral pH, GMP cannot usually compete with thiols for binding to Pt^{II} when both ligands are present at equal concentrations.[9] The kinetic preference of [Pt(dien)(H_2O)]$^{2+}$ at neutral pH is exclusively toward thiols when in competition with 5′-GMP.[9] Complex **1** increases steric crowding in the square plane and circumvents resistance caused by reactions with glutathione and other cellular thiols, but still maintains the ability to form cytotoxic lesions with DNA.[4] From the experimental results obtained above, the rate of binding of the thiol ligand GSH to complex **1** is greatly slowed but is still faster than that of 5′-GMP. Substitution of Cl^- by the thiol ligand appeared to proceed *via* prior aquation because of the steric hindrance by the 2-methylpyridine ligand. The presence of hydrolysis products in the system provides a pathway for the formation of mono- and bis-GMP adducts which are formed *via* hydrolysis steps. The bis(GMP) adduct was stable in the presence of free GSH even after 3 d, but was present in only small amounts.

Conclusion

Labelling of the new anticancer drug *cis*-[$PtCl_2$($^{15}NH_3$)(2-pic)] has allowed detailed insight to be gained into the kinetics and mechanisms of its reactions with 5′-GMP and glutathione. The steric effect of 2-picoline reduces the reactivity of complex **1** towards 5′-GMP compared to its 3-picoline analogue, especially towards substitution in the position *cis* to 2-picoline. The low reactivity of complex **1** towards 5′-GMP may explain why it forms interstrand DNA cross-links much more slowly than cisplatin.[2] Two HT isomers were observed for *cis*-[Pt($^{15}NH_3$)(2-pic)(5′-GMP-*N7*)$_2$]$^{2+}$ due to the slow rotation of 2-picoline and non-C_2-symmetrical structure. Reactions of GSH with complex **1** were *ca*. three times slower than those with **2**, and appeared to proceed *via* aquated intermediates, with initial binding of GS^- *trans* to 2-picoline for **1** and *trans* to NH_3 for **2**. The bis(GMP) adduct of complex **1** was able to form in the presence of GSH at neutral pH in a competitive reaction. The steric effect of 2-picoline and asymmetric structure of **1** may give rise to several isomers when it binds to DNA. This, together with its low reactivity towards GSH, may play an important role in its high activity against cisplatin-resistant cell lines.

Acknowledgements

This research was supported by the Biotechnology and Biological Sciences Research Council, Engineering and Physical Sciences Research Council (Biomolecular Sciences Programme), and EC COST programme. We are grateful to the Committee of Vice-Chancellors and Principals for an ORS Award, University of Edinburgh for a Research Studentship for Y. Chen and Johnson Matthey plc for the loan of some Pt.

References

1 J. Reedijk, *Chem. Commun.*, 1996, 801.
2 F. I. Raynaud, F. E. Boxall, P. M. Goddard, M. Valenti, M. Jones, B. A. Murrer, M. Abrams and L. R. Kelland, *Clin. Cancer Res.*, 1997, **3**, 2063.
3 J. Holford, S. Y. Sharp, B. A. Murrer, M. Abrams and L. R. Kelland, *Br. J. Cancer*, 1998, **77**, 366.
4 J. Holford, F. Raynaud, B. A. Murrer, K. Grimaldi, J. A. Hartley, M. Abrams and L. R. Kelland, *Anti-Cancer Drug Design*, 1998, **13**, 1.
5 Y. Chen, Z. J. Guo, S. Parsons and P. J. Sadler, *Chem. Eur. J.*, 1998, **4**, 672.
6 S. E. Miller and D. A. House, *Inorg. Chim. Acta*, 1989, **161**, 131.
7 F. Raynaud, F. Boxall, P. Goddard, M. Valenti, M. Jones, B. Murrer, C. Giandomenico and L. Kelland, *Proc. 88th Annual Meeting American Assoc. Cancer Res.*, San Diego, CA, 12–16 April 1997, vol. 38, no. 2085, p. 311.
8 Y. Zou, B. Van Houten and N. Farrell, *Biochemistry*, 1993, **32**, 9632.
9 R. N. Bose, S. Moghaddas, E. L. Weaver and E. H. Cox, *Inorg. Chem.*, 1995, **34**, 5878.
10 J. Reedijk, in *Handbook of Metal–Ligand Interactions in Biological Fluids*, ed. G. Berthon, Marcel Dekker, New York, 1995, vol. 2, p. 967.
11 T. Ishikawa, C. D. Wright and H. Ishizuka, *J. Biol. Chem.*, 1994, 29085.
12 S. J. S. Kerrison and P. J. Sadler, *J. Chem. Soc., Chem. Commun.*, 1977, 861.
13 S. J. Barton, K. J. Barnham, A. Habtemariam, P. J. Sadler and R. E. Sue, *Inorg. Chim. Acta*, 1998, **273**, 8.
14 M. Piotto, V. Saudek and V. Sklenar, *J. Biomol. NMR*, 1992, **2**, 661.
15 J. Stonehouse, G. L. Shaw, J. Keeler and E. D. Laue, *J. Magn. Reson., Ser. A*, 1994, **107**, 178.
16 E. W. Abel, T. P. J. Coston, K. G. Orrell, V. Sik and D. Stephenson, *J. Magn. Reson.*, 1986, **70**, 34.
17 S. J. Berners-Price and P. J. Sadler, *Coord. Chem. Rev.*, 1996, **151**, 1.
18 H. Friebolin, *Basic One- and Two-Dimensional NMR Spectroscopy*, VCH, Weinheim, 1991.
19 G. Pettit and L. D. Pettit, *IUPAC Stability Constants Database*, IUPAC and Academic Software, Otley, 1993.
20 F. Basolo, J. Chatt, H. B. Gray, R. G. Pearson and B. L. Shaw, *J. Chem. Soc.*, 1961, 2207.
21 D. F. Shriver, P. W. Atkins and C. H. Langford, *Inorganic Chemistry*, 2nd edn., Oxford University Press, 1994, p. 627.
22 R. Romeo, D. Minniti and M. Trozzi, *Inorg. Chem.*, 1976, **15**, 1134.
23 S. S. Eapen, M. Green and I. M. Ismail, *J. Inorg. Biochem.*, 1985, **24**, 233.
24 K. J. Barnham, S. J. Berners-Price, T. A. Frenkiel, U. Frey and P. J. Sadler, *Angew. Chem.*, 1995, **34**, 1874.
25 S. J. Berners-Price, K. J. Barnham, U. Frey and P. J. Sadler, *Chem. Eur. J.*, 1996, **2**, 1283.
26 D. Kiser, F. P. Intini, Y. Xu, G. Natile and L. G. Marzilli, *Inorg. Chem.*, 1994, **33**, 4149.
27 B. Lippert, *Prog. Inorg. Chem.*, 1989, **37**, 1.
28 M. D. Reily and L. G. Marzilli, *J. Am. Chem. Soc.*, 1986, **108**, 6785.
29 Y. Xu, G. Natile, F. P. Intini and L. G. Marzilli, *J. Am. Chem. Soc.*, 1990, **112**, 8177.
30 R. E. Cramer and P. L. Dahlstrom, *Inorg. Chem.*, 1985, **24**, 3420.
31 S. J. Berners-Price, U. Frey, J. D. Ranford and P. J. Sadler, *J. Am. Chem. Soc.*, 1993, **115**, 8649.
32 K. Inagaki, F. J. Dijt, E. L. M. Lempers and J. Reedijk, *Inorg. Chem.*, 1988, **27**, 382.
33 A. T. M. Marcelis, J. L. Van Der Veer, J. C. M. Zwetsoot and J. Reedijk, *Inorg. Chim. Acta*, 1983, **78**, 195.
34 K. Okamoto, V. Behnam, M. T. Phan Viet, M. Polissiou, J. Y. Gauthier, S. Hanessian and T. Theophanides, *Inorg. Chim. Acta*, 1986, **123**, L3.
35 J. F. Hartwig and S. J. Lippard, *J. Am. Chem. Soc.*, 1992, **114**, 5646.
36 A. J. Repta and D. F. Long, in *Cisplatin Current Status and New Developments*, eds. A. W. Prestayko, S. T. Crooke and S. K. Carter, Academic Press, New York, 1980, p. 285.
37 M. I. Djuran, E. L. M. Lempers and J. Reedijk, *Inorg. Chem.*, 1991, **30**, 2648.
38 B. J. Corden, *Inorg. Chim. Acta*, 1987, **137**, 125.
39 T. G. Appleton, J. W. Connor, J. R. Hall and P. D. Prenzler, *Inorg. Chem.*, 1989, **28**, 2030.
40 K. J. Barnham, M. I. Djuran, P. del S. Murdoch, J. D. Ranford and P. J. Sadler, *Inorg. Chem.*, 1996, **35**, 1065.
41 B. Odenheimer and W. Wolf, *Inorg. Chim. Acta*, 1982, **66**, L41.

Paper 8/06544F